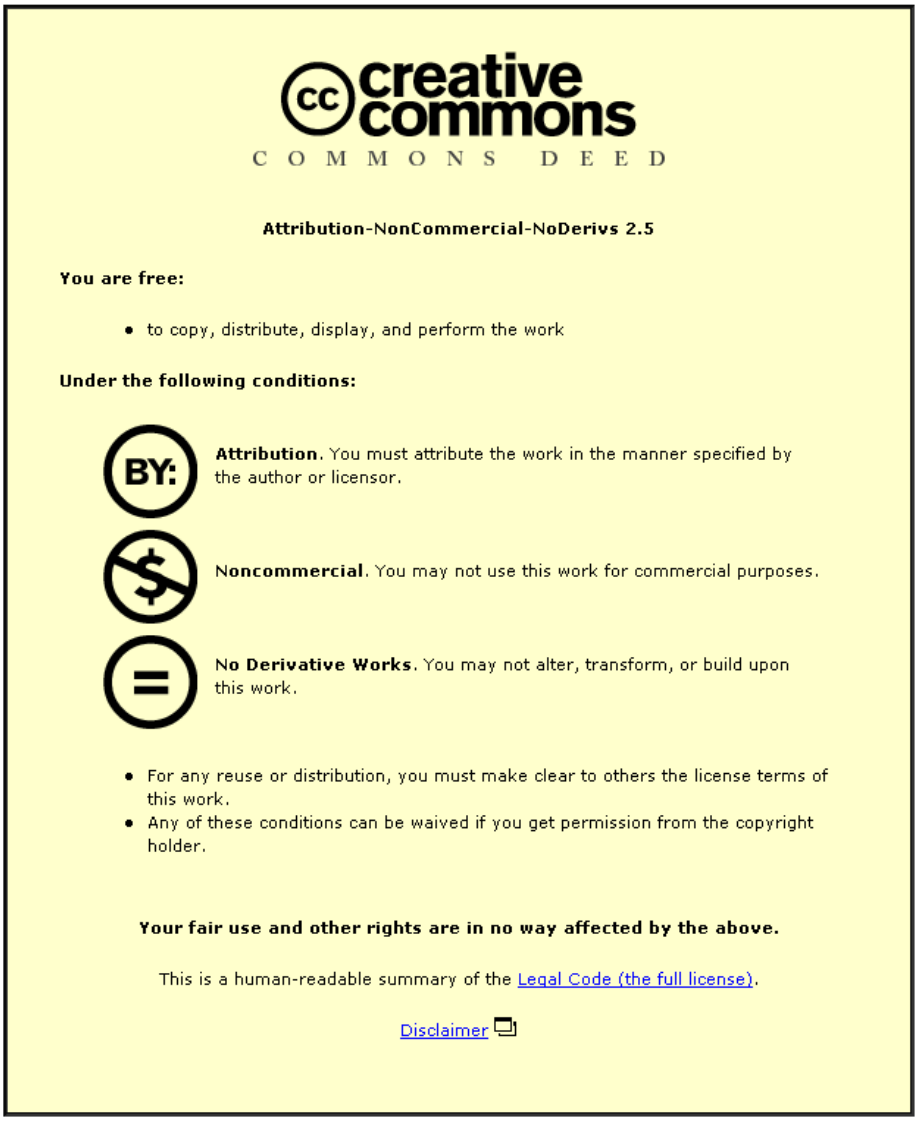

creative commons

COMMONS DEED

Attribution-NonCommercial-NoDerivs 2.5

You are free:

- to copy, distribute, display, and perform the work

Under the following conditions:

Attribution. You must attribute the work in the manner specified by the author or licensor.

Noncommercial. You may not use this work for commercial purposes.

No Derivative Works. You may not alter, transform, or build upon this work.

- For any reuse or distribution, you must make clear to others the license terms of this work.
- Any of these conditions can be waived if you get permission from the copyright holder.

Your fair use and other rights are in no way affected by the above.

This is a human-readable summary of the Legal Code (the full license).

Disclaimer

Excimer laser machining of bisphenol A polycarbonate under closed immersion filtered water with varying flow velocities and the effects on the etch rate

C F Dowding* and **J Lawrence**
Wolfson School of Mechanical and Manufacturing Engineering, Loughborough University, Loughborough, UK

The manuscript was received on 26 October 2009 and was accepted after revision for publication on 21 December 2009.

DOI: 10.1243/09544054JEM1869

Abstract: Until now, progress in laser ablation micromachining has been significantly limited with respect to feature miniaturization and output yield by ablation-generated debris. Gas-jetting techniques have proven to be inadequate and vacuum environments are unwieldy in an industrial setting. To this end, a controlled geometry for both the optical interfaces of a flowing liquid film can be provided by a closed flowing thick film filtered water immersion technique. This ensures repeatable machining conditions and allows control of liquid flow velocity. To investigate the impact of this technique on etch rate, bisphenol A polycarbonate samples have been machined using KrF excimer laser radiation passing through a medium of filtered water flowing at a number of flow velocities that are controllable by modifying liquid flowrate. A mean increase in etch rate of 8.5 per cent when using a turbulent flow velocity regime immersed ablation over ablation in ambient air was recorded. However, use of laminar flow velocities resulted in a mean loss of 26.6 per cent in etch rate compared to ablation in ambient air. Plotting the recorded etch rate achieved with respect to flow velocity gives support for previously proposed flow–plume interactions: the primary cause of a 37 per cent variance in etch rate over a 72 per cent change in laminar flow velocity was a shift in the ratio between the refresh rate of liquid volume over the feature and laser repetition rate. The small variance of etch rate achieved by modification of turbulent regime flow velocity indicates that laser etching provided the dominating contribution to the total etch rate measured. This work demonstrates that this technique developed for ablation debris control does not reduce the efficiency of laser etching with respect to that achieved with established gas media laser ablation machining. Therefore, this process shows great promise for industrial implementation development.

Q4 **Keywords:**

1 INTRODUCTION

1.1 Background and rational

Since the emergence of micro and nano manufacturing in the late 1970s, the technology has been continuously enhanced and improved upon [**1**–**3**]. Laser fluence, optical resolution, and production speed have been refined to such high levels that today it is the actual laser ablation-generated debris that is stymieing progress [**4**]. Debris can contribute to beam attenuation after ejection but before deposition [**5**] and can be generated in a mode that coats unimportant areas, areas still to be machined, or, worse still, features that have already been machined [**6**]. To compound matters, debris can coat machinery, requiring costly downtime for cleaning and servicing [**7**], or can become airborne in the working environment of tool users, posing potential respiratory health issues [**7**]. The use of a technique involving closed flowing thick film filtered water immersion of the sample during laser ablation has shown promise as a solution to such problems [**9**]; however, the impact of such techniques on the basic laser machining characteristics are not extensively documented.

**Corresponding author: Wolfson School of Mechanical and Manufacturing Engineering, Loughborough University, Loughborough, Leicestershire LE11 3TU, UK.*
email: colin_dowding@hotmail.com

1.2 Material use

The molecular structure of amorphous polymers, such as bisphenol A polycarbonate, causes them to respond well to laser ablative machining [**10**]. Yet despite the high etch rates achievable, multiple large monomers are ejected to be deposited back onto the substrate surface following machining, causing debris issues. The high visibility of deposited laser ablation-generated debris, coupled to the good laser ablation removal characteristics of amorphous polymer materials makes Bisphenol A polycarbonate an excellent candidate material for assessment of in-line debris control techniques. The performance of the control technique both for debris control and its impact on the machining process can be easily assessed using this material.

1.3 Current ablation theory

The ablation rate is useful to the observer as it is an easily measured technique for quantifying the efficiency of coupling between a photon stream and a material once above the threshold fluence – an event well known to be a probabilistic [**11**]. Ablation is a complex phenomenon with many contributing components [**12**]. A number of mechanisms are cited: shockwaves instigated by the high pressures achieved inside the ablation plume cause mechanical damage of the material [**13**]; high temperatures achieved inside the ablation plume in combination with the action of the laser beam cause thermal attack of the surface [**14**, **15**]. A prediction technique of the action of these etch mechanisms, either alone or in a combination thereof has been created by Prasad *et al.* [**16**].

1.4 Previous liquid immersed laser ablation machining

Work has been conducted to investigate the effect of open thin-film immersion on the ablation rate of excimer laser ablation of bisphenol A polycarbonate. A number of limitations were observed and causes diagnosed. Splashing was a common occurrence during machining. This was attributed to irregular but broadly increased plume pressure, as identified by Berthe *et al.* [**17**], which significantly attenuates the laser beam en route to the sample surface [**18**]. When using open thin-film immersion, the necessary volume of liquid is not available to confine the ablation plume pressure; thus, a threshold pressure exists in this condition; once exceeded, rupture occurs and plume gas escapes violently from the covering liquid film into the ambient air above, producing liquid splashing as a by-product [**19**]. Furthermore, surface ripple occurred and hence the depth of liquid above the plume varied with respect to time and position above the sample, resulting in an irregular and non-repeatable plume etch-rate. This was demonstrated by the ablation depth with respect to pulse number ratio fluctuations from the expected linear trend [**18**, **19**], given the regular, repeatable surrounding medium used.

This technique aims to remove this problem by enclosing the flow in a sealed duct. The use of a closed flow chamber guarantees optical geometry of the medium surrounding the sample by fully confining the boundaries of the flow passing through the ducting. As well as this, confinement of all boundaries guarantees symmetrical drag levels about the centre planes of the flow. Flow eddies, as given schematically in Fig. 1(a), are dominated by a parameter known as the characteristic distance, as has been previously experimented with [**9**, **18**, **19**]. In an open flow, turbulence commences following a characteristic distance measured between the contact point of a fluid on a flat plate and the point at which the flow becomes turbulent [**20**]; however, this case

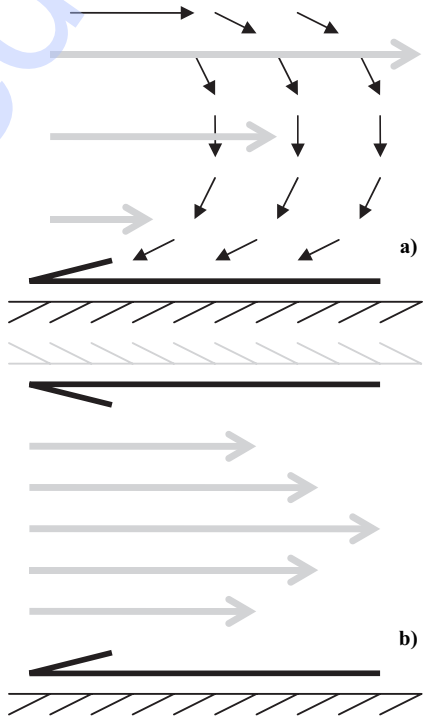

Fig. 1 Schematic showing the effect of differing boundary conditions on flow turbulence: open flow causes an uneven drag profile, generating rolling turbulence in the manner described by the black vectors: (a) generation of turbulence always occurs after a characteristic flow displacement, dependent upon fluid properties; (b) closed flow allows symmetrical drag profile, generating a flow velocity profile similar to that described by the grey arrows. The generation of turbulence is dependent upon flow velocity; laminar flowrates do not generate turbulent flow at any point

requires all dimensions of the flow, including film depth, to be large compared to the characteristic distance. In the case of an open flow, the meniscus defines the flow geometry; thus, the effects of rolling eddies alone are not responsible for the deposition patterns evidenced by Dowding and Lawrence [**9**], where debris distribution appeared to lie in ripple patterns downstream of the feature machined. Instead, large inertial, capillary, and viscous contributions complicated the flow path. This work applies a closed geometry (forming a duct) to give a symmetrical drag profile across the cross-section of the flow as drawn in Fig. 1(b). This means that the characteristic distance of a closed flow is determined by the cross-sectional dimensions of the duct and the meniscus domination of open flows is avoided. This allows laminar flows to be achieved at low flowrates [**20**]. Also, the maintenance of a repeatable and regular containment of the surrounding medium allows the importance and action of liquid flow velocity on the fundamental ablation characteristics of liquid immersion to be investigated by varying the flow velocity and measuring the results.

1.5 Research goals

Previous work has successfully demonstrated the application of closed thick film flowing liquid immersion as a means of controlling ablation generated debris during the laser ablation machining process [**21**], while producing high-quality features, as can be seen in Fig. 2. The process must also be characterized in terms of its impact on laser etching performance. This work will explore the impact of closed flowing thick film filtered water immersed laser ablation machining using KrF excimer laser radiation on the ablation rate of bisphenol A polycarbonate. This will be compared to that achievable by KrF ablation machining in ambient air. Further, the importance of liquid flow velocity to the ablation rate will be explored in detail in this work. Etch rate offers an accessible indication of the machining effectiveness and efficiency of a laser ablation process. If these are significantly modified from that recorded in ambient air, a modification to the ablation mechanism is the likely cause.

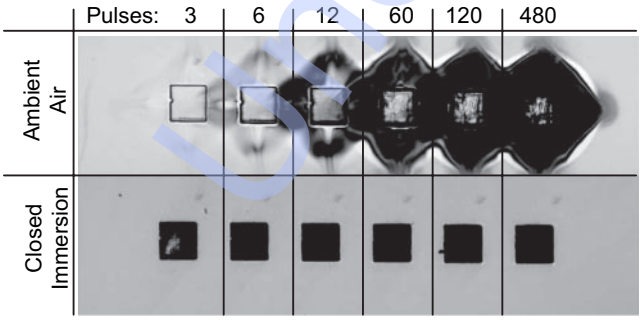

Fig. 2 Two rows of KrF excimer laser machined features, each machined using the number of pulses indicated, (a) in ambient air, and (b) using closed thick film flowing filtered water immersion of the sample

2 EXPERIMENTAL PROCEDURES

2.1 Material details

Bisphenol A polycarbonate (Holbourne Plastics Ltd), was as received in $1200 \times 1000\,\mathrm{mm}^2$ sheets of 0.5 mm thickness. Prior to excimer laser processing, the bisphenol A polycarbonate sheet was cut into rectangular sections of $8 \times 12\,\mathrm{mm}^2$ using scissors – a shear cutting technique which avoids production of debris. Protective cover sheets were then peeled off each sample.

2.2 Laser details and experimental set-up

For both closed flowing thick film filtered water immersion and ambient air processing, an excimer laser (LPX200; Lambda Physique, GmbH) using KrF as the excitation medium was used to produce a beam with a wavelength of 248 nm. Thereafter, the beam was supplied to a laser micromachining centre (M8000; Exitech Ltd), where it was passed through a stainless steel mask to produce a $201 \times 203\,\mu\mathrm{m}^2$ rectangular image. The masked beam was then demagnified through a $4\times$ optic (Francis Goodhall Ltd) to produce an ablation spot with a depth of focus (DoF) of 6 μm. A profile of the masked beam was obtained using a beam profiler (SP620U; Spiricon Ltd), which showed that the beam shape had an even distribution, with only a slight positive skew across the *y* axis; demonstrating good positioning of the mask in the raw beam.

A sample included six machined sites, each produced using increasing numbers of pulses (3, 6, 12, 60, 120, 480) in the same machine run with uninterrupted filtered water flow over the sample during machining. The beam was attenuated by a tool attenuator set at 126° from minimum transmission, resulting in a beam fluence of $581\,\mathrm{mJ/cm}^1$ and $578\,\mathrm{mJ/cm}^1$ for ablation in ambient air and under filtered water immersion respectively, that produced features of $203 \times 205\,\mu\mathrm{m}^2$. This fluence data was calculated from pulse energy data taken using a pulse energy head (J50LP-2, Molectron Detector, Inc.) positioned above the focal point of the laser, and enumerated by a laser energy meter (EM400, Molectron Detector Inc.). The fluence was calculated using the mean beam energy measured (averaging techniques were employed for experimental rigour: beam pulse energy was recorded five times before and after machining each sample, every value recorded was

the mean value measured over 100 pulses – between readings the attenuator was reset to account for attenuator position errors) so that any changes in laser output over time were accounted for.

2.3 Ambient air laser processing

Samples machined in ambient air were produced, using the same laser and micromachining equipment as the closed flowing thick film filtered water immersion ablation samples. The bisphenol A polycarbonate samples were mounted directly to the vacuum chuck inside the micromachining station (M8000, Exitech Ltd). After lasing ended, the sample was removed and placed into the cell of a sealed sample tray to protect it from atmospheric dust.

2.4 Closed thick-film filtered water immersion laser processing procedure

Figure 3(a) describes the critical experimental layout of the sample once clamped inside the flow rig, which was mounted to the side of the sample vacuum chuck of the laser micro-processing centre (M8000; Exitech Ltd). The sample was positioned in the centre of the flat aluminium table between the water supply and exit holes. The sample was retained by a recess in a spacer plate (to provide a 1.5 mm-thick water film) that lay in contact with the aluminium sample table. An O-ring cord, located by a rectangular groove in the sample table, provided a seal between the sample table and the spacer plate. On top of the spacer plate a second oval O-ring groove was machined to locate another O-ring cord. This acted as a gasket between the spacer plate and the beam window – a $25 \times 25 \times 5\,\text{mm}^3$ ultra-violet grade fused silica sheet (Comar Instruments Ltd). The beam window was retained by a diamond-shaped recess in a third aluminium plate, 8 mm in thickness to provide stiffness to the whole sandwich. The use of a closed ablation chamber removes the variance of the flow geometry both with respect to time and position above the sample to be machined. If a thin-film regime closed flowing immersion technique (less than 1.1 mm in thickness [**21**]) is implemented, the compressed ablation plume will extend through the flowing liquid from the sample surface to the bottom surface of the chamber window potentially plume etching the window, damaging a critical component in the optical path of the beam. This means that the experiments conducted in this work used a thick film regime to prolong the life of the chamber window.

Figure 3(b) shows the water filtering and supply system. Water originated from a normal mains supply by wall tap. The water was poured into a domestic water filter (Britta Inc.) situated at the top of the water supply assembly to remove typical corrosive elements present in mains water. The water was then

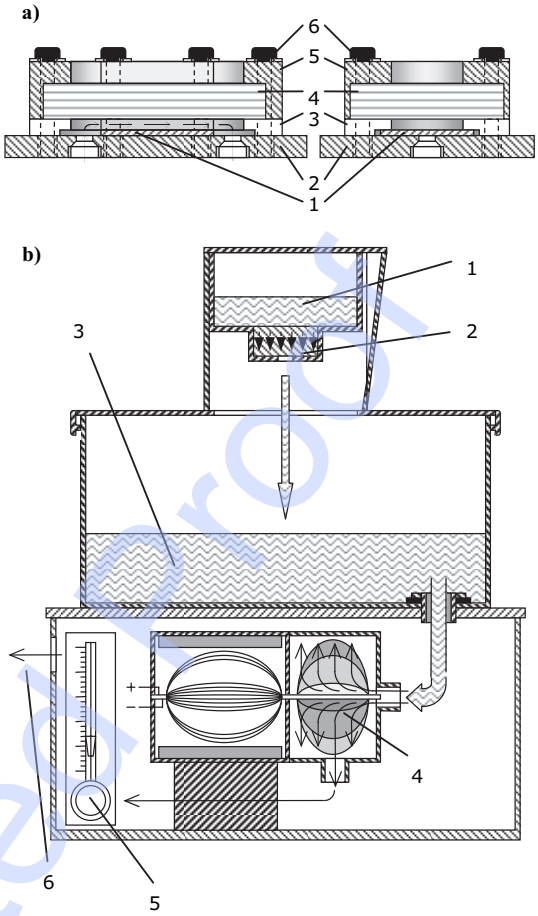

Fig. 3 Schematic showing assemblies of (a) the sample manifold: sample (1); base plate (2); sample clamp and flow chamber spacer (3); UV grade fused silica window for laser beam (4); window clamp (5); clamping bolts that squeeze components together (6); and (b) the fluid supply unit: source water (1); filtering (2); filtered water storage (3); centrifugal pump (4); flowrate control valve (5); high pressure flowrate controlled filtered water outlet to flowrate ablation chamber (6)

retained in a header tank located above the pump and, under the action of gravity, was forced into the 700 W pump chamber (CPE100P, Clarke Power Products Ltd). The pump forced the water through a water flowrate metre (FR4500, Key Instruments Inc.) and then along a 3 m distance through a 6 mm outer diameter nylon tube to the inlet push-in elbow fitting on the bottom of the sample table. Last, the water was returned along a further 3 m through a 6 mm outer diameter nylon tube to a collection bucket. The pump was capable of producing 4.2 bar at the outlet, equating to a maximum flow velocity through the ablation chamber of 3.89 m/s, given losses along the supply and return tubing. Precise control of the flow velocity was provided by a variable valve of the flow meter. Flow velocities of 0.03, 0.11, 1.39, 2.31, 2.78, and 3.24 m/s were used for this work.

2.5 Sample analysis techniques

The ablation depths were measured using a dragged needle profiler (CM300 Talysurf; Taylor-Hobson Ltd). Five passes were made across the surface of the sample and into each feature at 50 μm intervals. To minimize the possibility of profile error, the mean average depth of each sample feature was then calculated from a selection of three profiles for each sample feature. To guard against outlier samples being produced and affecting the ablation threshold measurements taken, all data plotted for interpretation in these results are mean average values taken from the data produced by three sample features machined using each flow velocity.

3 RESULTS AND DISCUSSION

3.1 Modification of media surrounding the ablation event

Comparison of the mean etch rate achieved by KrF laser ablation under closed thick-film laminar flow velocity regime filtered water immersion and in ambient air is given by Fig. 4. The mean plot of ablation under closed thick-film laminar flow velocity regime filtered water immersion is given with error bars indicating the 37 per cent difference between the two flow velocities used. The mean etch rate of these two is plotted by a long dashed linear trend line in Fig. 4, giving a mean etch rate of 115.2 nm/pulse. Ambient air is plotted without error bars as all the features used to measure the mean ablation rate were machined into a matrix of features in one machine run; thus, the laser fluence, measured to be a mean value of 581 mJ/cm^2, is taken to be uniform for all feature groups. The etch rate recorded for KrF excimer laser ablation of bisphenol A polycarbonate in ambient air was 144.7 nm/pulse. The mean etch rate achieved by KrF laser ablation under closed thick-film laminar flow velocity regime filtered water immersion is 20 per cent lower than the ablation rate achieved in ambient air. The error bars given in Fig. 4 indicate that the etch rate in a laminar flow would not exceed that of ambient air in any case.

The mean performance of KrF excimer laser ablation immersed under closed thick film turbulent flow velocity regime filtered water can be compared, in Fig. 4, to the performance of a beam measured to have a fluence of 581 mJ/cm^2, making this comparable to the beam used for samples machined in ambient air. The plot points of the mean etch rate generated under turbulent flow filtered water include the 9 per cent error bars required to represent the 2 per cent variance of the measured fluences of the beams used to machine the turbulent flow samples and the 7 per cent range from highest to lowest recorded etch rate. Inspection of this plot shows that the mean etch rate centre line, indicated by the small dashed linear trend line in Fig. 4, is 13 nm/pulse greater than that of ablation in ambient air; this is an 8.5 per cent increase in etch rate when using closed thick-film turbulent flow velocity regime filtered water immersed ablation over ablation conducted in ambient air.

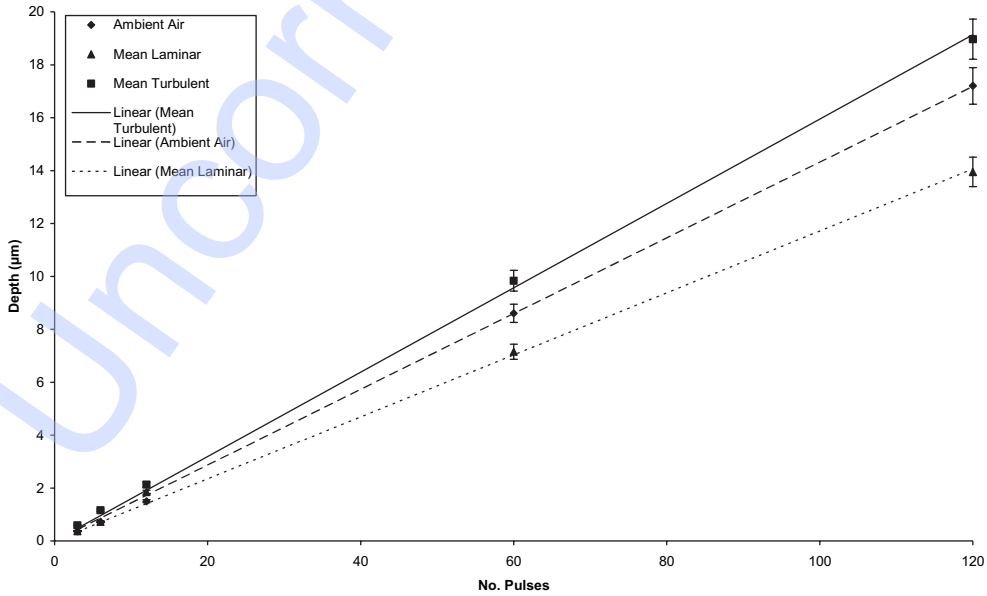

Fig. 4 Graph plotting the mean closed thick film immersed ablation etch depth achieved with respect to the number of laser pulses under laminar and turbulent regime flow velocities are offered for comparison with samples machined using ablation in ambient air

3.2 Impact of flow velocity on ablation depth

The variance of fluid velocity used for closed thick-film flowing filtered water immersion for removal of machining debris during laser ablation has a direct impact on the etch rate achieved. The clearest demonstration of this is given graphically in Fig. 5: the feature depth achieved using a nominal number of laser pulses, identified in the plot legend, through the immersing closed thick-film filtered water. First, the depth achieved is proportional to the number of pulses fired, which is an expected and logical result: every pulse removes material; thus, the cumulative effect of '*n*' pulses will be approximately '*n*' multiplied by the etch depth of a single pulse, for 3, 6, 12, 60, and 120 pulses, this linear relationship is borne out. As an example, examining the depths machined at 2.78 m/s gives 0.512, 1.046, 2.205, 10.03, and 19.25 μm. However, the use of 480 pulses, does not follow this trend; instead, the depth etched is 36.65 μm, a value that falls below the expected depth given the relationship described above. When machined, there was no allowance made in the stage control algorithm to correct beam optical length as the feature was machined ever deeper (this could be done by moving the sample towards the de-magnifying optic by the single pulse etch depth after every pulse). Figure 5 illustrates that the bottom of the machined feature falls out of the focal range of the micromachining system between 120 and 480 pulses. Therefore, with this knowledge, the rest of this work will not include 480 pulses in the calculation of etch rates. More significant to this work, the simple plot of feature depth with respect to immersing liquid flow velocity given in Fig. 5 demonstrates that low flow velocities cause '*n*' pulses to machine less material than high flow velocities. A rapid but smooth increase in etch depth generated by '*n*' pulses is followed through the laminar flow velocities (0 to 0.27 m/s), through intermediate flow velocity (0.27 to 0.47 m/s) and into the turbulent region (0.47 m/s and upwards). The results show that once using turbulent flow velocities there is little increase in etch efficacy.

3.3 Impact of flow velocity on etch rate

The ratio determined by comparing the number of pulses used to machine a measured feature depth gives the etch rate, that is, the mean depth machined by a laser beam at a measured fluence in a single pulse [**11**]. Figure 6 gives three plots. The plot described by the solid black linear trend line is the mean of all the etch rates measured in the turbulent flow velocity regime; this plot is listed to act as a reference for the two plots of interest in Fig. 6. Two flow velocities were used in the laminar regime: 0.03 and 0.11 m/s. However, the laser repetition rate was increased by a multiple of four to 200 Hz for the 0.03 m/s sample. This was done with the intention of raising the pulse repetition rate above the frequency that the volume of liquid covering the feature is completely renewed. This was to generate a potential for debris to remain suspended above the feature as the following pulse arrived. The samples machined at the flow velocity of 0.11 m/s all had a fluence within 3 per cent of 579 mJ/cm^2, as indicated by the error bars in Fig. 6. The linear trend line for 0.11 m/s flow velocity is marked by a close dashed line and gives an

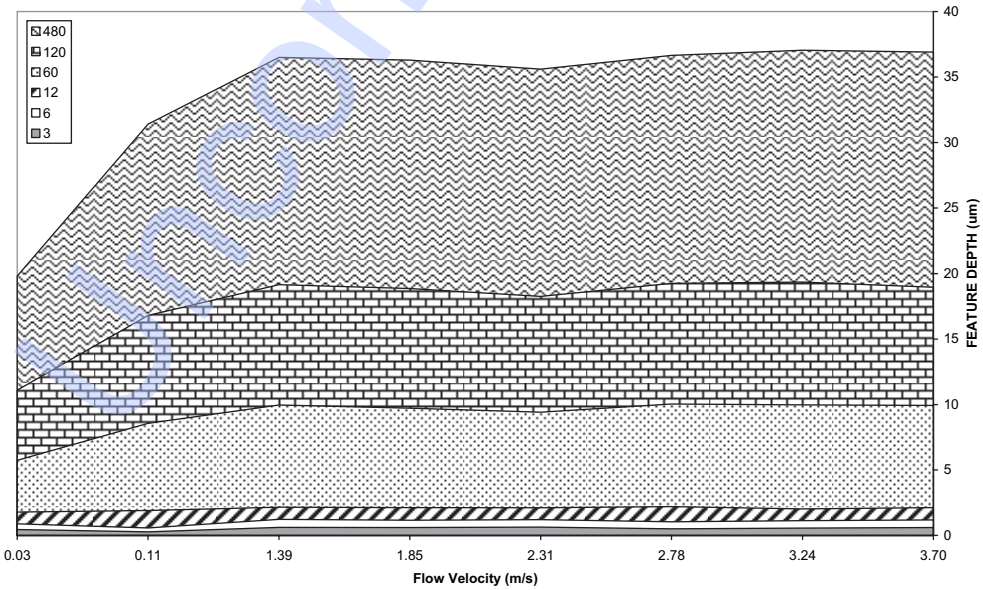

Fig. 5 Filled line graph plotting the depth machined by 3, 6, 12, 60, 120, and 480 pulses at 0.03, 0.11, 1.39, 1.85, 2.31, 2.78, 3.24, and 3.70 m/s

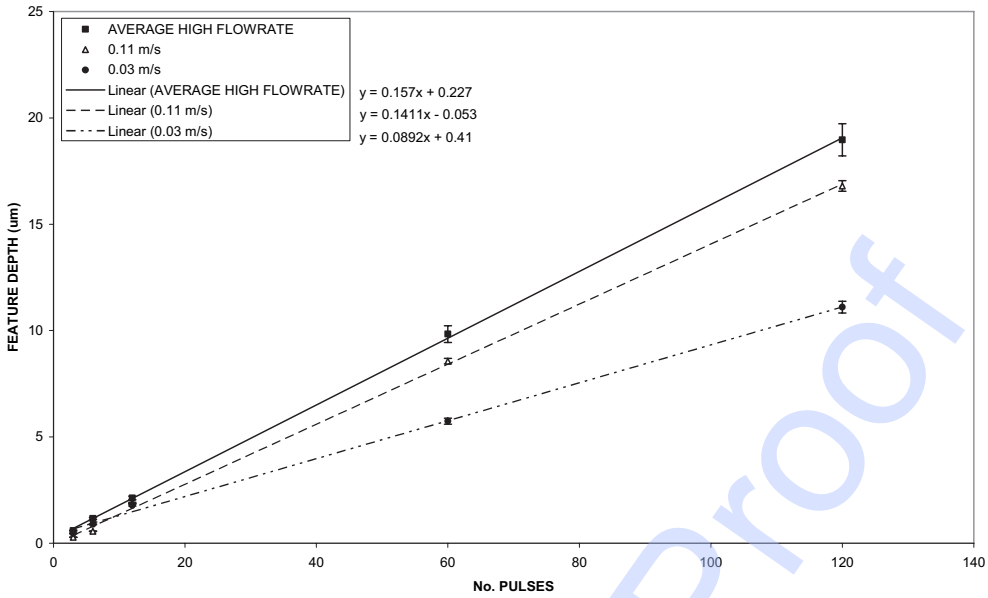

Fig. 6 Graph plotting the mean depth against the number of pulses used under turbulent regime flow velocity closed thick film immersion for comparison with that achieved by laminar flow regime closed thick film filtered water immersion flow velocities of: 0.03 and 0.11 m/s

etch rate of 141.1 nm/pulse, thus giving a decrease in etch rate of 15.9 nm/pulse, a drop of 10 per cent from that achieved by mean ablation under a closed thick film turbulent flowing filtered water immersion. The samples machined for the 0.03 m/s flow velocity were all machined using a beam fluence within 4 per cent of 578 mJ/cm^2. The trend for 0.03 m/s flow velocity is represented by a double – dot – dashed linear line that has a gradient of 89.2 nm/pulse, a value that is 43 per cent lower than the etch rate achieved under a turbulent velocity filtered water flow and 37 per cent lower than the etch rate achieved using a flow that was 72 per cent slower than the 0.11 m/s laminar flow velocity. The difference between the two laminar flow velocities is marked compared to that between 0.11 m/s and the turbulent flow velocities. This is caused by a dramatic change in the refresh rate of the immersing fluid over the machined feature. This must be compared to the pulse repetition rate of the laser. For the 0.11 m/s sample the repetition rate of the laser was 50 Hz and the refresh rate of the immersing filtered water was 556 Hz, giving a ratio of 11.1 new liquid volumes between laser pulses, compared to a ratio of 0.695 new liquid volumes between laser pulses as the liquid volume was only refreshed 139 times every second for the 0.03 m/s flow velocity. Clearly, this significant disparity has resulted directly in a marked reduction of etch rate.

In Fig. 7 the etch rate of a laser beam were measured to be within 2 per cent of 578 mJ/cm^2 for every sample machined (as indicated by error bars), therefore allowing the etch rates plotted for each closed thick-film filtered water immersion flow velocity to be compared. Figure 7 demonstrates that the turbulent flow velocities used (1.39 to 3.70 m/s separated by increments of 0.46 m/s) made little difference to the etch rate of bisphenol A polycarbonate using KrF excimer laser pulses. This fact is demonstrated by the gradients in the equations listed for each flow velocity in Fig. 7. These gradients, which are equivalent to the numerical etch rates of the material, vary by just 7 per cent of the lowest etch rate achieved (measured as 150.2 nm/pulse, achieved at 2.31 m/s). These results cover a range of liquid volume refresh rate with respect to laser repetition rate ratios of 231 (an increase of 167 per cent over the lowest turbulent velocity used); this marks a large ratio range with little modification to etch rate compared to the response demonstrated when using laminar regime flow velocities, as discussed above. This is an interesting contrast in trends, indicating a complex and potentially useful relationship between the flowing immersion liquid and the ablation plume.

3.4 Flow–plume interaction states: the action of flow velocity on laser ablation

The dashed line in Fig. 8 represents the etch rate of the closed thick film flowing filtered water immersed samples and the solid, horizontal line represents the etch rate measured for the samples machined in ambient air. Use of a range of flow velocities in a closed thick film flowing filtered water immersion ablation technique has resulted in a distinct trend that is described graphically in Fig. 8. These two plots clearly demonstrate the change in typical etch rate at laminar flow velocities that drop sharply beneath the

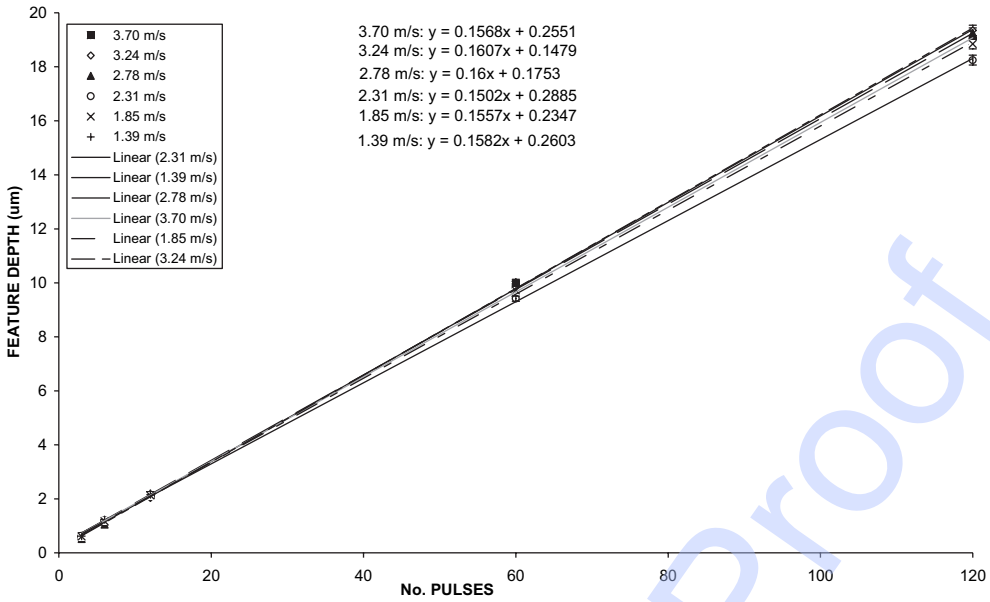

Fig. 7 Plots describing the relationship between etch depth and number of laser pulses for five turbulent regime flow velocities: 1.39, 1.85, 2.31, 2.78, 3.24, and 3.70 m/s

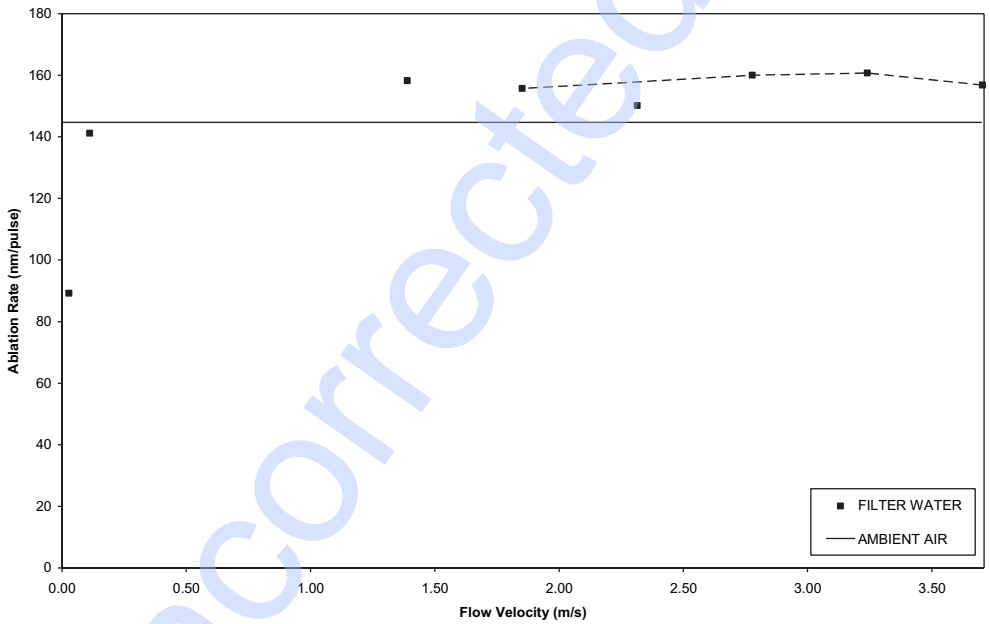

Fig. 8 Ablation rates measured are plotted with respect to liquid flow velocity for ablation conducted under closed thick film flowing filtered water immersion and in ambient air

etch rate produced in ambient air to a trend that follows a high power law, smoothing with increasing flow velocity. This can be explained by the interaction of the flowing liquid and the debris suspended within that flow on the laser beam and the ablation plume generated. At very low flow velocities, where the ratio of fluid volume refresh rate with respect to laser repetition rate is less than 1, debris particles that were ejected from the machined feature in all directions, including upstream, were still suspended in the flow above the entirety of the feature when the following pulse arrived. These particles intercepted the beam en route to its destination, lowering the fluence of the beam arriving at the feature, as described in Fig. 9(a), reducing the etching efficiency of the laser energy originally delivered by the laser. This is a result plotted schematically in Fig. 10, which also identifies that a threshold level of laser etching is

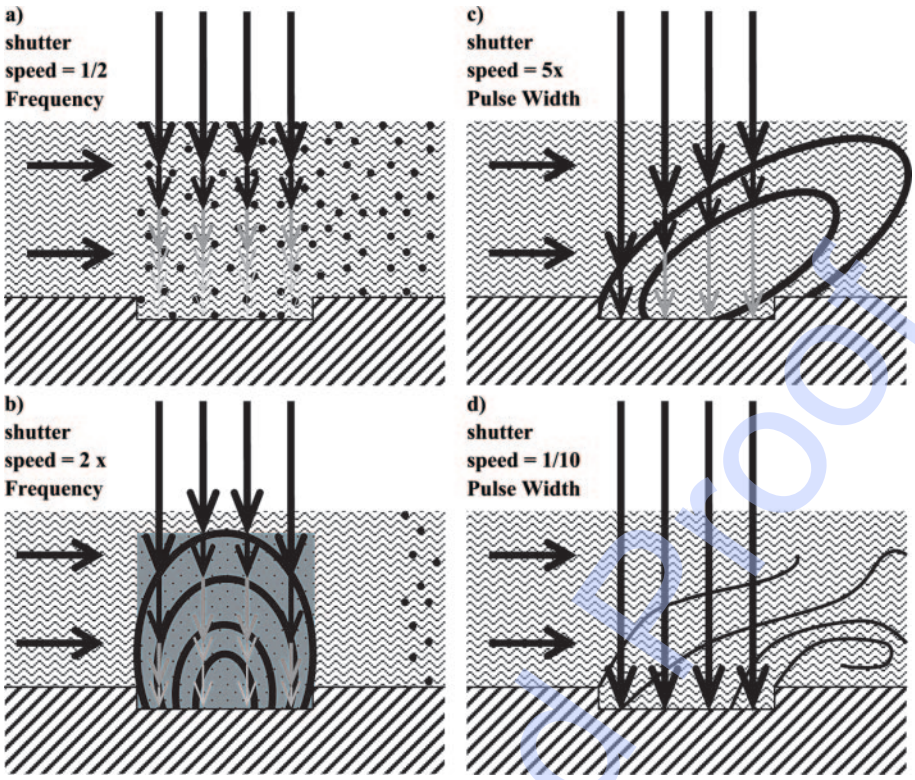

Q5

Fig. 9 Schematic showing flow – plume interaction states when: (a) the flowrate is laminar and the laser pulse frequency is high, thus the following pulse is intercepted by remaining suspended debris; (b) increased flow velocity beneath the optimum allows the ablation plume to fully develop, maximizing plume attenuation while compensating by uninhibited plume etching; (c) an optimum condition occurs when the flowing liquid distorts the ablation plume to minimize plume attenuation without removing the action of plume etching; (d) very high flow velocity with respect to the pulse width results in distortion of the ablation plume by the viscous fluid

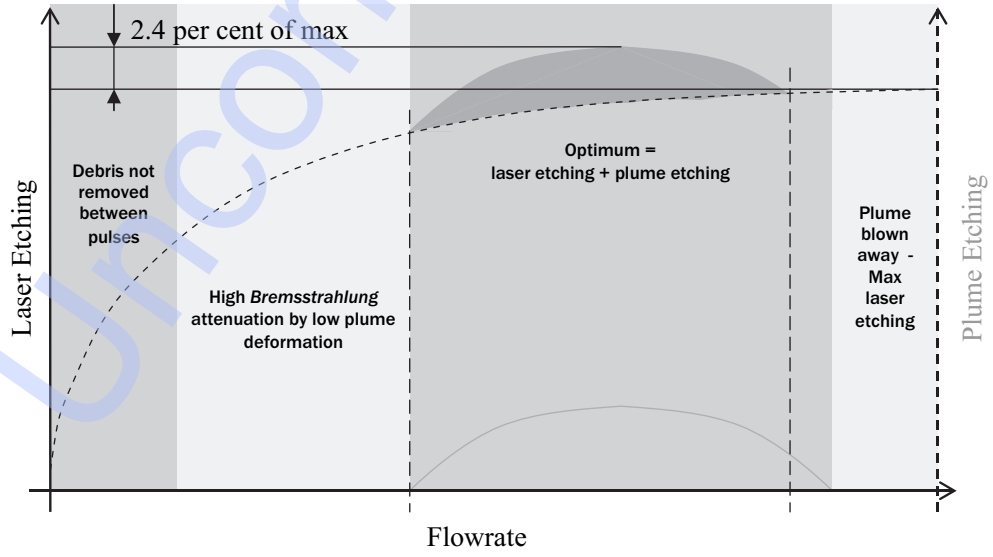

Fig. 10 Schematic plot showing the action and combination of plume etching and laser etching and the flow velocity dependence of both. An optimum point exists and is depicted by the dashed vertical line, where the summation of both etching mechanisms combines to maximum effect

required to instigate a plume to add a contribution to the etching. As the frequency ratio between laser repetition rate and fluid volume refresh rate increased past 1 to 11.1, the debris was removed from the site of the machined feature before the second pulse arrived. This left the full quota of beam fluence to pass onto the sample surface; except that the highly viscous nature of the immersing filtered water constrained the expansion of the ablation plume. The flow was still not rapid, as it was travelling in the laminar regime, and was not travelling with sufficient velocity to distort the ablation plume which expanded over a short timeframe within the flow as described schematically in Fig. 9(b). This compressed ablation plume has a greater optical density when immersed in filtered water than it does in ambient air, causing the immersed ablation plume to provide increased attenuation to the continuing laser pulse by means of shockwave refraction [**22**], Mie scattering [**23**], Rayleigh scattering [**24**], and *Bremsstrahlung* attenuation [**25**] when compared to the situation of ablation in ambient air, reducing the laser energy arriving at the sample surface. However, some etching contribution was given by the ablation plume, reducing this perceived hindrance [**17**, **21**, **28–30**] as denoted schematically in Fig. 10, where the plume has now been allowed to develop and begins to aide in the etching process, although the laser etching possible is still not optimum.

As the flow velocity moves into the turbulent regime, the ablation plume begins to become distorted and lean due to the drag on it imparted by the rapid flow velocity of the high viscosity flow past it. This reduced the optical path length of the ablation plume for the laser beam as described schematically in Fig. 9(c). The plume was merely distorted in shape at this point, and could still provide a significant etching contribution. At some flow velocity, shown in Fig. 8 to be between 2.78 and 3.24 m/s, the distortion of the plume reached a maximum before the flow velocity became so high that it began to destroy the plume and reduce the plume-etching contribution. This was the optimum etch-rate point, where the laser had good access to the material and the plume is still etching effectively, and is indicated in Fig. 10 by the dashed line. In Fig. 10 the accumulative effect of laser etching and plume etching is presented in the grey area at the top of the diagram.

Q1 3.70 m/s is shown to have a reduced ablation rate compared to that measured at 3.24 m/s in Fig. 8. The cause of this is illustrated in Fig. 9(d); the flow velocity was so rapid that it was destroying the ablation plume before it was able to become fully developed and provide an etching contribution, however the lack of an ablation plume means that the laser beam has almost unopposed access to the material surface. This point is plotted to the right of Fig. 10. Figure 10 is also useful in describing the criticality of the two etching processes. Figure 8 shows that the peak ablation rate was only 2.4 per cent larger than that of samples machined at non-optimum turbulent flow velocities; this value is marginal, but critically, larger than the maximum experimental error calculated to be 2 per cent. This is because the contribution of plume etching is small compared to that of laser etching, as indicated by the schematic plot in Fig. 10.

4 CONCLUSIONS

The etch rate achieved using 3, 6, 12, 60, and 120 pulses shows a linear relationship between etch depth and number of shots. Use of 480 pulses resulted in an etch depth significantly lower than that predicted by the linear relationship followed by the lower pulse numbers, demonstrating that the feature was being machined to a depth outside the extents of the focal range of the micromachining system as the algorithm used to machine these samples did not correct the sample height between pulses. More importantly, it was shown that etch depth increased rapidly with flow velocity through the laminar flow velocity regime, and became more stable in the turbulent velocity regime.

A 20 per cent reduction in etch rate was measured when using laminar flow velocity immersion of laser ablation with closed thick film filtered water when compared to that produced by a similar KrF excimer laser beam with a fluence of 581 mJ/cm^2 ablating bisphenol A polycarbonate in ambient air. The mean etch rate measured when laser ablation machining under a turbulent flow velocity regime closed thick film filtered water flow was 8.5 per cent greater than that achieved by ablating with a similar KrF excimer laser beam in ambient air using a fluence of 581 mJ/cm^2.

As suggested by the previous inspection of etch depth with respect to flow velocity, analysis of the etch rate generated by flow velocities of 0.03 and 0.11 m/s, both being laminar regime velocities, during closed thick film flowing filtered water immersed KrF excimer laser ablation of bisphenol A polycarbonate showed that modification of flow velocity in the laminar flow velocity regime causes large variance of the etch rate. Moreover, inspection of the flow velocity with respect to traverse distance of the flow over the feature required to provide a refreshed volume of water over the feature between laser pulses is important. At 0.03 m/s the filtered water volume above the feature was refreshed 0.695 times between laser pulses and 11.1 times at 0.11 m/s. This means that the lower velocity flow could not remove suspended debris generated by one laser pulse from above the sample before the arrival of the next; this

suspended debris intercepted the oncoming pulse before it arrived at the intended destination, reducing effective laser fluence at the feature. This is in contrast to the high laminar flow velocity, where the debris is completely removed from above the sample and the laser beam has clear access to the feature for machining. This effect is a critical component in the 37 per cent variance between the two laminar flow velocities. Comparison of the mean etch rate achieved in a laminar regime flow shows a 26.6 per cent reduction in etch rate to that achieved in a turbulent regime flow. Detailed analysis of the etch rates produced at six turbulent regime flow velocities (1.39, 1.85, 2.31, 2.78, 3.24, and 3.70 m/s), using a beam fluence of $578 \pm 5.78\,\mathrm{mJ/cm^2}$ every flow velocity tested, highlighted, and quantified the small variance in etch rate of 7 per cent generated by modification of the flow velocity in the high velocity flow regime. This is a small modification to ablation rate given the large variation in flow velocity; a large contrast to the trend shown at laminar flow velocities.

Comparison of the etch rates measured with the flow velocities they were machined in shows a trend that confirms that suggested by the initial analysis of etch depth with respect to flow velocity. The trend also supports a scenario of flow–plume interactions previously proposed. When suspended debris was not removed between pulses due to insufficient flow velocity, the following pulse was intercepted by the suspended debris. Next, the flow velocity was sufficiently high to remove debris from above the feature between pulses, but insufficient to distort the ablation plume during a pulse. The immersion of the ablation plume with filtered water restricted the expansion of the plume, resulting in a plume of increased optical and physical density compared to that produced by ablation in ambient air. This compressed plume attenuates the laser beam producing the plume, reducing the beam energy that arrives at the material and as a result, the etch rate. At the same time, the compressed plume reduced the loss in etch rate by the action of plume etching. Increased flow velocity resulted in the production of an optimum etch rate, where the plume was distorted by the flowing filtered water, reducing the path length that the beam had to endure through the plume to reach the material surface, and as a result the losses due to plume attenuation are lower. Simultaneously, the distorted, but still intact ablation plume was still providing a plume etching contribution. Further increased flow velocity began to destroy the ablation plume, allowing maximum access to the material surface for the beam and removing the plume-etching contribution. The small variance of etch rate achieved by modification of turbulent regime flow velocity indicates that laser etching provided the dominating contribution to the total etch rate measured.

REFERENCES

1 **Rizvi, N. H.** and **Apte, P.** Developments in laser micromachining techniques. *J. Mater. Proc. Technol.*, 2002, **127**, 206–210.
2 **Dyer, P. E.** Excimer laser polymer ablation: twenty years on. *Applied Phys. A*, 2003, **77**, 167–173.
3 **Gower, M. C.** Excimer laser microfabrication and micromachining. Laser precision microfabrication. *RIKEN Review*, 2001, 50–56.
4 **Braun, A., Zimmer, K., Hösselbarth, B., Meinhardt, J., Bigl, F.,** and **Mehnert, R.** Excimer laser micromachining and replication of 3D optical surfaces. *Applied Surf. Sci.*, 1998, **127–129**, 911–914.
5 **Izatt, J. A., Sankey, N. D., Partovi, F., Fitzmaurice, M., Rava, R. P., Itzkan, I.,** and **Feld, M. S.** Ablation of calcified biological tissue using pulsed hydrogen fluoride laser radiation. *IEEE J. Quantum Electron.*, 1990, **26**(12), 2261–2270.
6 **Ghantasala, M. K., Hayes, J. P., Harvey, E. C.,** and **Sood, D. K.** Patterning, electroplating and removal of SU-8 moulds by excimer laser micromachining. *J. Micromech. Microengng*, 2001, **11**, 133–139.
7 **Lankard, J. R.** and **Wolbold, G.** Excimer laser ablation of polyimide in a manufacturing facility. *Applied Phys. A*, 1992, **54**, 355–359.
8 **Lobo, L. M.** *Solid phase by-products of laser material processing*, Doctoral Thesis, 2002, Loughborough University.
9 **Dowding, C. F.** and **Lawrence, J.** Use of thin laminar liquid flows above ablation area for control of ejected material during excimer machining. *Proc. IMechE Part B: J. Engng Mf.*, 2009, **223**(6), 759–774.
10 **Jang, B. N.** and **Wilke, C. A.** The thermal degradation of bisphenol A polycarbonate in air. *Thermochimica acta*, 2004, **246**(1–2), 73–84.
11 **Crafer, R.** and **Oakley, P. J.** *Laser processing in manufacturing*, 1993 (Chapman & Hall, London).
12 **Georgiou, S.** and **Koubenakis, A.** Laser-induced material ejection from model molecular solids and liquids: mechanisms, implications, and applications. *Chem. Rev.*, 2003, **103**(2), 349–394.
13 **Pataulf, G.** and **Dyer, P.** Photomechanical processes and effects in ablation. *Chem. Rev.*, 2003, **103**(2), 487–518.
14 **Lee, S. K., Chang, W. S.,** and **Na, S. J.** Numerical and experimental study on the thermal damage of thin Cr films induced by excimer laser irradiation. *J. Applied Phys.*, 1999, **86**(8), 4282–4289.
15 **Kelly, R.** and **Miotello, A.** On the role of thermal processes in sputtering and composition changes due to ions or laser pulses. *Nuclear instruments and methods in physics research section b: beam interactions with materials and atoms*, 1998, **141**(1–4), 49–60.
16 **Prasad, M., Conforti, P. F.,** and **Garrison, B. J.** Coupled molecular dynamics-Monte Carlo model to study

the role of chemical processes during laser ablation of polymeric materials. *J. Chem. Phys.*, 2007, **127**(8), 127–139.

17 **Berthe, L., Fabbro, R., Peyre, P.,** and **Tollier, L.** Shock waves from a water-confined laser-generated plasma. *J. Applied Phys.*, 1997, **82**(6), 2826–2832.

18 **Dowding, C. F.** and **Lawrence, J.** Analysis of the excimer laser ablation characteristics of bisphenol A polycarbonate in ambient air and under thin film laminar flow water immersion. In Proceedings of the 27th International Congress *on Application of Lasers and Electro-Optics: Laser Materials Processing Section*, 2008, 202–211.

19 **Dowding, C. F.** and **Lawrence, J.** Impact of open deionized water thin film laminar immersion on the liquid immersed ablation threshold and ablation rate of features machined by KrF excimer laser ablation of bisphenol A polycarbonate. *Opt. Lasers in Enng*, 2009, **47**(11), 1169–1176.

20 **Munson, B. R., Donald, F. Y.,** and **Theodore, H. O.** *Fundamentals of fluid mechanics*, 2002, vol. 4 (John Wiley & Sons Inc., New York).

21 **Dowding, C. F.** and **Lawrence, J.** Ablation debris control by means of closed thick film filtered water immersion. *Proc. IMechE Part B: J. Engng Mf.*, accepted for publication 24 September 2009.

22 **Nahen, K.** and **Vogel, A.** Shielding by the ablation plume during Er:YAG laser ablation. *Proc. SPIE*, 2001, **4257**, 282–297.

23 **van de Hulst, H. C.** *Light scattering by small particles*, 1957 (John Wiley & Sons, Inc. USA).

24 **Schittenhelm, H., Callies, G., Straub, A., Berger, P.,** and **Hügel, H.** Measurements of wavelength-dependent transmission in excimer laser-induced plasma plumes and their interpretation. *J. Applied Phys.*, 1998, **31**, 418–427.

25 **Faenov, A. Y., Magunov, A. L., Pikuz, T. A., Skobelev, I. Y., Pikus, S. A., Bollanti, S., DiLazzaro, P., Lisi, N., Flora, F., Letardi, T., Palladine, L., Reale, A., Scafati, A., Grilli, A., Batani, D., Mauri, A., Osterheld, A.,** and **Goldstein, W.** Characteristics of plasma heating by short wavelength excimer laser radiation. *Kvantovaya Elektronika*, 1996, **23**(8), 719–724.

26 **Zhu, S., Lu, Y. F., Hong, M. H.,** and **Chen, X. Y.** Laser ablation of solid substrates in water and ambient air. *J. pplied Phys.*, 2001, **89**(3), 2400–2403.

27 **Fabbro, R., Peyre, P., Berthe, L.,** and **Scherpereel, X. L.** Physics and applications of laser-shock processing. *J. Laser Applic.*, 1998, **10**(6), 265–269.

28 **Elaboudi, I., Lazare, S., Belin, C., Talaga, D.,** and **Labrugere, C.** Underwater excimer laser ablation of polymers. *Applied Phys. A*, 2008, **92**(4), 743–748.

29 **Elaboudi, I., Lazare, S., Belin, C., Talaga, D.,** and **Labrugere, C.** From polymer films to organic nanoparticles suspensions by means of excimer laser ablation in water. *Applied Phys. A*, 2008, **93**(4), 827–831.

30 **Elaboudi, I., Lazare, S., Belin, C., Talaga, D.,** and **Labrugere, C.** Organic nanoparticles suspensions preparation by underwater excimer laser ablation of polycarbonate. *Applied Surf. Sci.*, 2007, **253**(13), 7835–7839.